ACS APPLIED POLYMER MATERIALS

Editors' Choice
Open Access

pubs.acs.org/acsapm

Article

Design of Side-Chain Fluorinated Polyethers Featuring Predefined Breaking Points for Fluorosurfactant Applications

Tom Reimers, Larissa Limmer, Gregor M. Linden, Johannes Liermann, Reiner Friedrich, and Holger Frey*

Cite This: ACS Appl. Polym. Mater. 2026, 8, 5101−5114

Read Online

ACCESS | Metrics & More | Article Recommendations | Supporting Information

ABSTRACT: Fluorosurfactants are an integral part of many industrial processes due to their unparalleled surface activity and high water and oil repellency and can be found in a wide range of consumer products. However, their lack of biodegradability causes great environmental concern and has led to increased regulatory action in recent years. In the search for alternatives, perfluoropropyl vinyl ether was recently identified as a promising building block with an improved ecological profile regarding degradation and accumulation. Here, we utilized short-chain perfluoropropyl vinyl ether (PPVE) or perfluoromethyl vinyl ether (PMVE) as precursors to construct polyether-based fluorosurfactants through copolymerization with hydrophilic comonomers. Surfactant properties and overall fluorine content per molecule could be easily adjusted by changing the comonomer feed. The surface activity was investigated in aqueous solution via tensiometry and was found to be competitive with both legacy PFAS such as perfluorooctanesulfonic acid and current state-of-the-art small molecule fluorosurfactants ($\gamma_{stat} \geq 20.35$ mN m^{-1}). These findings illustrate the potential of amphiphilic copolymers as a modular, straightforward, and versatile platform for next-generation fluorosurfactants as an alternative to long-chain legacy PFAS.

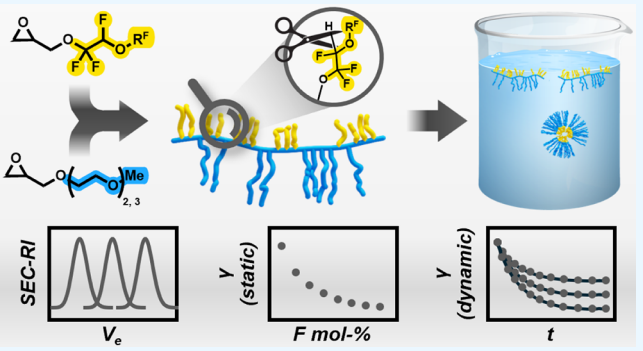

KEYWORDS: *fluorosurfactants, surface tension, PFAS, side-chain fluorinated polymers, polyethers, degradability*

INTRODUCTION

Organofluorines have emerged as an essential class of materials in modern industry, with applications ranging from nonstick coatings,[1] water- and dirt-repellent coatings for outdoor clothing,[2] as surfactants,[3] stabilizers in paints[4] or in firefighting foams.[5] Fluorosurfactants used as stabilizers and emulsifiers in organic reactions can allow to omit organic solvents[6] and enable emulsion polymerizations.[7] All these uses have their origin in the low polarizability of fluorine, which leads to low interactions with aqueous as well as organic surroundings. Fluorosurfactants are typically more efficient than their hydrocarbon homologues. They show lower surface tension and critical micelle concentrations (CMC) due to their increased stiffness, surface area, and decreased interactions.[3,5] As a result of the strong carbon−fluorine bond, the compounds furthermore exhibit excellent thermal and chemical stability.[5,8] While this may be desirable and targeted for some applications, their persistence has become an ecological problem. Per- and polyfluorinated substances (PFAS) are detected all over the world[9] and are accumulating in the food chain,[10] with some PFAS also showing toxicity.[11,12] A majority of the PFAS used today are still based on long-chain perfluorinated carbon chains such as perfluorooctanoic acid (PFOA) or perfluorooctanesulfonic acid (PFOS), which are facing increased regulations and are in urgent need of alternatives.[13−16] Because of their exceptional properties, it is challenging to find nonfluorinated replacements, and thus, degradable and nontoxic PFAS are in focus of studies.[5,13] Two strategies were introduced to develop fluorinated alternatives: small-chain PFAS and long-chain PFAS with an incorporated ether linkage as a breaking point. Small-chain PFAS show reduced bioaccumulation,[17] but are still persistent in the environment.[18] Long-chain ether-bearing PFAS are degradable to small-chain PFAS using highly energy-consuming processes like high-temperature incineration,[19] electrochemical oxidation,[20] ultrasonication with strong oxidants[21] or oxygenation in subcritical water,[22] but generally show no biodegradation under environmentally relevant conditions.[10] Consequently, there is a high demand for fluorosurfactants with an improved degradation profile. This is especially true for applications with increased environmental exposure, such as aqueous fire-

Received: January 13, 2026
Revised: March 9, 2026
Accepted: March 9, 2026
Published: March 27, 2026

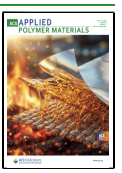

Table 1. Overview of Selected PFAS Recently in Focus of Studies, Featuring −O−CHF− or −S−CHF− Structural Motifs for Facilitated Biodegradation

Name	Structure	IUPAC name, CAS registry number	References
ProFdiEOH	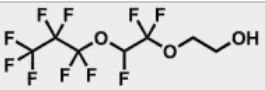	2-(1,1,2-trifluoro-2-(perfluoropropoxy)ethoxy)ethan-1-ol 640731-94-8	28,31,32
FESOH	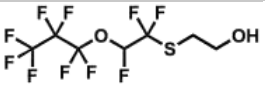	2-((1,1,2-trifluoro-2-(perfluoropropoxy)ethyl)thio)ethan-1-ol	24–26,28,31–35
MeFdiEOH	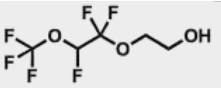	2-(1,1,2-trifluoro-2-(trifluoromethoxy)ethoxy)ethan-1-ol	28,31,32
MeFESOH	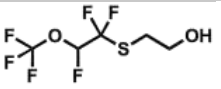	2-((1,1,2-trifluoro-2-(trifluoromethoxy)ethyl)thio)ethan-1-ol	28,31,32
PFC_3GE	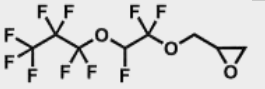	2-((1,1,2-trifluoro-2-(perfluoropropoxy)ethoxy)methyl)oxirane	This work, 29,36
PFC_1GE	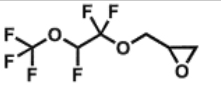	2-((1,1,2-trifluoro-2-(trifluoromethoxy)ethoxy)methyl)oxirane	This work, 29,36

fighting foams (AFFF)[5] or (architectural) paints and coatings.[23]

Recently, it was found that an increase in reactivity can be achieved by combining an ether linkage with a neighboring carbon−hydrogen bond, enabling degradation of certain PFAS such as FESOH and proFdiEOH (Table 1) under environmental conditions. Joudan et al. investigated a fluorosurfactant based on FESOH and found it to undergo degradation in the atmosphere as well as in activated sludge to perfluoropropionic acid (PFPrA).[24,25] Similarly, Folkerson et al. found the same surfactant to be transformed to PFPrA as the terminal product of rat metabolism.[26] Notably, relatively fast elimination rates with half-lives in the order of hours were observed, whereas most legacy PFAS are well-known for their tendency to bioaccumulate and their inertness toward metabolization.[27] Recently, Sadrabadi et al. observed that these polyfluoroether compounds do not induce PPARα-mediated toxicity or disrupt lipid metabolism in human liver cells, suggesting a favorable toxicological profile compared to legacy PFAS.[28]

Inspired by these findings, we developed epoxy-bearing compounds PFC_3GE and PFC_1GE by combining the polyfluorinated motifs from ProFdiEOH and MeFdiEOH with a glycidyl unit as reactive functional group available for further modification (Table 1).[29] We envision these compounds to serve as degradable alternatives to conventional fluorinated epoxides due to the −O−CHF−CF_2− motif as an initial point for degradation. Notably, due to their high ring strain of 110−115 kJ/mol, epoxides are ideal monomers for polymer synthesis via ring-opening polymerization techniques.[30]

Long-chain PFAS, particularly C8-based structures, generally outperform their short-chain homologues due to their higher fluorine content per molecule, which enhances surfactant properties.[37] In contrast, short-chain fluorinated moieties are more environmentally benign but offer lower individual performance.[38] Thus, incorporating short-chain PFAS multiple times in a polymeric structure provides an efficient strategy to increase the overall fluorine content per macromolecule while preserving the intrinsic short-chain character of each unit.[35] Here, we aimed to investigate whether polymeric surfactants composed of short-chain PFAS could match or even surpass the performance of long-chain analogues through a potential synergistic effect. Crucially, while the degradability of FESOH, ProFdiEOH and similar small-molecule PFAS has been thoroughly investigated (Table 1), it is yet unclear how attaching such structures to a polymer backbone affects degradation kinetics. To this end, a detailed investigation of the degradation process must be conducted, which will be the focus of future studies.

In this work, polyether-based fluorosurfactants were synthesized by copolymerizing fluorinated monomers PFC_3GE or PFC_1GE with suitable hydrophilic comonomers via monomer-activated anionic ring-opening polymerization (MAROP). Surface activity of the copolymers was achieved via mutual orientation of hydrophilic and amphiphobic (fluorinated) segments, leading to amphiphilic behavior of the overall structure. As hydrophilic components, epoxides bearing oligo (ethylene glycol) side chains ME_3GE or ME_2GE, respectively, or mPEG macroinitiators were employed (Figures 1 and 2). The polymer microstructure of all statistical copolymers was

https://doi.org/10.1021/acsapm.6c00173
ACS Appl. Polym. Mater. 2026, 8, 5101−5114

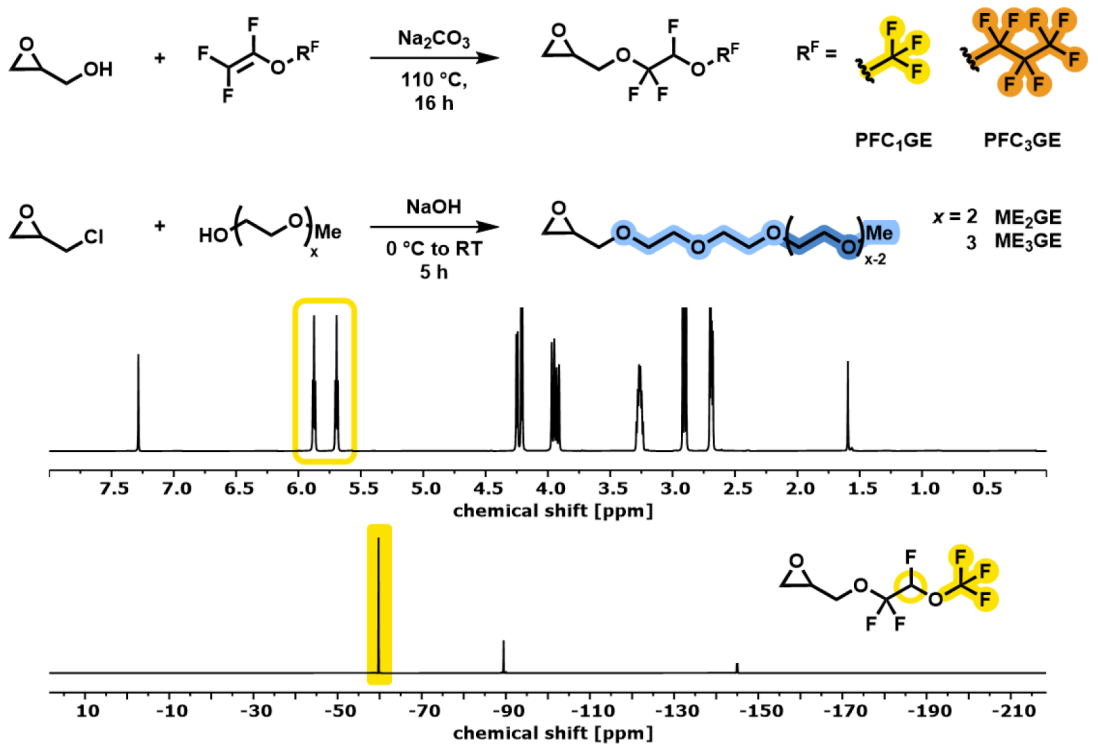

Figure 1. Synthetic pathways toward fluorinated and hydrophilic epoxide-based monomers utilized in this study (top) as well as exemplary ^{1}H NMR and ^{19}F-NMR spectra of PFC_1GE (bottom).

investigated using *in situ* ^{1}H NMR kinetic studies to assess the distribution of hydrophilic and amphiphobic side chains along the polymer backbone. All polymers were analyzed for their surfactant performance by measuring the static and dynamic surface tension, using the Wilhelmy method and the maximum bubble pressure method, respectively. Finally, proof-of-concept degradation tests employing basic chemical conditions were conducted to verify the polymers' susceptibility to chemical breakdown.

EXPERIMENTAL SECTION

Materials and Methods

All syntheses were conducted on a dual manifold vacuum-Argon Schlenk line unless specified otherwise

PFC_3GE was provided by Merck KGaA. PMVE was obtained in >99% purity from Chemours; diethylene glycol monomethyl ether was obtained in 99% purity from TCI; triethylene glycol monomethyl ether was obtained in >97% purity from Sigma-Aldrich. Tetrabutylammonium bromide (TBAB) was obtained in >98% purity from Alfa Aesar. Triisobutylaluminum (TIBAL) was obtained as a 1.1 M solution in toluene from Acros Organics. All remaining chemicals were purchased from Acros Organics, Fisher Scientific, Roth, Sigma-Aldrich, TCI, VWR, or Deutero GmbH. Chemicals were used as received unless specified otherwise.

Synthesis of PFC_1GE

The synthesis of PFC_1GE was adapted from a previously published patent.[29]

A 300 mL dried pressure-reactor was evacuated and flushed with argon three times. Potassium carbonate (0.3 eq, 2.80 g, 20 mmol), dioxane (5 eq, 28.7 mL), and glycidol (1 eq, 4.97 g, 67 mmol) were added. Glycidol was dried over calcium hydride for 2 h under cooling to prevent autopolymerization and distilled prior to use. The reactor was closed and evacuated. Gaseous PMVE was added thrice over 1.5 h until a constant pressure of 4.8 bar was established. The reaction mixture was stirred for a total of 16 h at 110 °C and then cooled to room temperature. The reactor was opened to release the excess PMVE into a slurry of calcium chloride (0.75 M) and potassium hydroxide (0.5 M). After flushing the reactor with nitrogen, 30 mL of water and 30 mL methyl *tert*-butyl ether were added and the mixture was transferred to a separatory funnel. The phases were separated, the organic phase was washed twice with water and once with brine and dried over sodium sulfate. The solvent was removed under reduced pressure and the product isolated via repeated fractional distillation (b.p.: 25 °C, 7 mbar). It is noted that complete removal of dioxane was impeded by extensive azeotrope formation, occasionally causing trace amounts of solvent to remain in the product mixture. PFC_1GE was obtained as a colorless liquid with a yield of 53% (8.67 g, 36.1 mmol).

Synthesis of ME_3GE and ME_2GE

The synthesis of *ME_3GE* is based on a procedure described by Wang et al.[39]

Epichlorohydrin (74 mL, 937 mmol, 3.0 equiv) and finely ground sodium hydroxide (37.7 g, 937 mmol, 3.0 equiv) were added to a 250 mL round-bottom flask equipped with a dropping funnel, and the suspension was cooled to 0 °C. Over a period of 30 min, triethylene glycol monomethyl ether (50 mL, 312 mmol, 1.0 equiv) was added dropwise and the mixture was stirred for 5 h at room temperature. Excess sodium hydroxide was removed by repeated vacuum filtration and the filtrate was dried over magnesium sulfate. Vacuum distillation yielded the product ME_3GE as a colorless liquid (55.5 g, 81%, b.p.: 97−102 °C at 0.020 mbar).

ME_2GE was synthesized following the same procedure as given above for ME_3GE. Final vacuum distillation gave ME_2GE as a colorless liquid with a yield of 87% (52.3 g, b.p.: 70 °C at 0.025 mbar).

Exemplary Synthesis of P(PFC_3GE_4-*co*-ME_3GE_{12}) Surfactant via MAROP

Tetrabutylammonium bromide (TBAB, 1 eq, 0.15 g) in 6 mL benzene was added to a dried Schlenk flask and dried under reduced pressure for 16 h. All additions were done via syringe. TBAB was suspended in 4 mL 2-methyltetrahydrofuran (2-MeTHF) and the

https://doi.org/10.1021/acsapm.6c00173
ACS Appl. Polym. Mater. 2026, 8, 5101−5114

flask was filled with argon. The monomers PFC_3GE (4 eq, 0.63 g) and Me_3GE (12 eq, 1.23 g) were added and the flask was cooled to 30 °C using an ethanol-nitrogen bath. Triisobutylaluminum (1.1 M in toluene, 2 eq, 0.85 mL) was added. When full conversion was indicated via ^{1}H NMR spectroscopy (typically after 2−16 h), the polymerization was terminated by addition of 1 mL of methanol. Triisobutylaluminum and TBAB residue was removed via liquid−liquid extraction using DCM (25 mL) and water (5 mL) five times. DCM was removed *in vacuo* and the sample was dried in the vacuum oven for at least 24 h, which gave the polymer as a colorless, viscous liquid in quantitative yield.

Exemplary Synthesis of $mPEG_{13}$-*b*-$P(PFC_3GE)_{13}$ Surfactant via MAROP

In a flame-dried Schlenk flask, mPEG 550 (1 eq, 0.43 mmol, 0.25 g) and KO*t*Bu (0.95 eq, 0.41 mmol, 46 mg) were dissolved in 1 mL methanol and 6 mL benzene and stirred for 3 h at 60 °C. The solvents were removed *in vacuo* overnight at 50 °C. The mixture was briefly heated to 60 °C under vacuum, after which 2-MeTHF (4 mL) and PFC_3GE (13 eq, 0.56 mmol, 1.17 mL) were added under argon atmosphere. PFC_3GE was freshly dried by distilling from CaH_2 and stored over 4Å molecular sieves under argon atmosphere prior to use. The mixture was cooled to −20 °C and Triisobutylaluminum (1.1 M in toluene, 2.2 eq, 0.86 mL) was added. The mixture was slowly allowed to reach r.t. and stirring was continued for 4 days. After polymerization, 1 mL of methanol was added and all volatiles were removed *in vacuo*. DCM (30 mL) was added and Triisobutylaluminum and TBAB residue were removed via extraction with D.I. water (5 x 10 mL). Solvents were removed and the product was obtained after final drying under vacuum at 50 °C.

In Situ ^{1}H NMR Kinetic Investigations

An exemplary procedure for online ^{1}H NMR kinetic analysis is described in the following. TBAB (10 eq, 0.11 mmol, 34 mg) in 3 mL benzene was added to a Schlenk flask and dried under reduced pressure. All following steps were done under argon atmosphere or vacuum using the Schlenk technique. TBAB was dissolved in 1 mL dry benzene, of which 0.1 mL (1 equiv) were added to a dried Norell S5400 NMR tube. The NMR tube was further equipped with a flame-sealed acetoned_6 capillary used for locking and shimming the NMR spectrometer. Benzene was removed under reduced pressure and TBAB dissolved in a dry, nondeuterated solvent (either 2-MeTHF or THF) and TIBAL (1.1 M in toluene, for polymerization in 2-MeTHF: 2 eq, 0.02 mL; in THF: 19 eq, 0.18 mL). The tube was shaken to homogenize the solution, cooled to 80 °C to prevent initiation and the monomers ME_3GE (24 eq, 0.25 mmol, 55.8 mg) and PFC_3GE (12 eq, 0.13 mmol, 43 mg) were added. The NMR tube was sealed by a Teflon stopcock and the mixture was only allowed to thaw immediately before the measurement was conducted. The tube was shaken beforehand to ensure homogeneity. The measurement was done at 10 °C for 6 h. Sample spinning was turned off. If the system was not able to lock on acetone-d_6, lock was turned off and shim was performed using the solvents signal. Spectra were recorded every 30 s.

Degradation Experiments

Degradation experiments were performed on $P(PFC_1GE)_8$ as a model polymer. The polymer (1eq, 0.12 g, 0.06 mmol) and diethylenetriamine (31 eq, 0.2 mL, 1.85 mmol) were dissolved in DMSO-d_6 (0.8 mL) and added to an NMR tube. The mixture was heated to 120 °C and decomposition of the fluorinated motifs was monitored via frequent ^{19}F NMR spectroscopy. Degradation experiments using KOH as a base were performed analogously. Here, precipitation of fluoride salt was observed in the course of the reaction.

■ ANALYTICAL METHODS

NMR Spectroscopy

NMR spectra were recorded on a *Bruker Avance III HD 300* instrument with a field strength of 300 MHz (^{1}H NMR), 75.5 MHz (^{13}C NMR) or 282 MHz (^{19}F NMR). The instrument was equipped with a 5 mm BBFO probe head with *z*-gradient and ATM. DOSY experiments as well as *in situ* NMR kinetic measurements were performed on a *Bruker Avance III HD 400* spectrometer. This instrument featured a 5 mm nitrogen-cooled BBO cryo probe head (BB/H+F) with *z*-gradient and ATM. The chemical shifts are specified by the devices relative to the signals of corresponding standards (tetramethylsilane for ^{1}H and ^{13}C measurements and trichlorofluoromethane for ^{19}F measurements). The chemical shifts of the signals in ppm are referenced to the solvent signal. Degradation experiments were monitored on a Magritek Benchtop NMR Spectrometer.

SEC (Size Exclusion Chromatography)

SEC measurements were performed on an *Agilent 1100 Series* system. HEMA (pore size 300/100/40 Å) was used as the column material in a column with a length of 95 cm and a width of 0.80 cm. The measurements were performed at a temperature of 50 °C with a flow rate of 1 mL/min and *N*,*N*-dimethylformamide as the eluent, to which 1 g/L lithium bromide was added as an association preventative. An RI detector was used to detect eluted species. The device was calibrated against PEG standards from Polymer Standards Services (PSS). The injection volume was 100 μL. As part of the sample preparation, approximately 3 mg of the sample was dissolved in approximately 1 mL of DMF and the solution was filtered through a syringe filter. A drop of toluene was added as an internal standard.

MALDI-ToF (Matrix-Assisted Laser Desorption/Ionization Time-of-Flight) Analysis. MALDI spectra of polymer samples were recorded on a *Bruker MALDI-ToF MS Autoflex maX* with a smartbeam II Nd:YAG laser (355 nm). The samples consisted of 10 μL of a 1 g/L analyte solution in DCM, to which 10 μL of a 10 g/L dithranol (DIT) matrix solution and 1 μL of a 0.1 M solution of sodium trifluoroacetate (NaTFA) or potassium trifluoroacetate (KTFA) as cationization reagent. The spectra were evaluated using the open source program *mMass*.

Static Surface Tension

Equilibrium surface activity was measured using the Wilhelmy plate method (DIN EN 14370) on a model *DCAT 11 tensiometer* from DataPhysics, Filderstadt, Germany. 0.1 wt % aqueous solutions were measured at 20 ± 0.2 °C using a 19.9 mm platin plate. Full wetting was ensured to eliminate the contact angle from the equation used for calculations: $\gamma_{stat} = F \cos\theta\, L^{-1} \approx FL^{-1}$ (γ = tension, F = tension force, θ = contact angle, L = wetted plate length).

Dynamic Surface Tension

Dynamic surface activity was determined via the bubble pressure method. For this, 0.1 wt % aqueous solutions were measured at 21 ± 0.9 °C using a model T60 tensiometer from SITA, Dresden, Germany. The dynamic surface tension was calculated using the equation $\gamma_{dyn} = r(p_{max} - \rho gh)2^{-1}$ (γ = tension, r = capillary radius, p_{max} = pressure maximum, ρ = liquid density, g = gravity, h = immersion depth).

DSC (Differential Scanning Calorimetry)

DSC measurements were performed using a DSC250 from TA Instruments (New Castle, DE, USA) with an RCS 90 compressor and using the TRIOS software. Calibration was performed using Indium and *n*-octane standards. Samples were prepared by weighing 3−5 mg of predried polymer in an Alumimum pan. The pan was sealed with an Aluminum lid,

https://doi.org/10.1021/acsapm.6c00173
ACS Appl. Polym. Mater. 2026, 8, 5101−5114

Table 2. Polymer Characterization Data and Static Surface Tension γ_{stat} of the Synthesized Polyether-Based Fluorosurfactants

No.	Polymer[a]	DP(A):DP(B)th[b]	x_F[a] [x_F^{th}]/%	w_F[a] [w_F^{th}]/%	M_n[c] [M_n^{th}]/g mol^{-1}	$Đ$[c]	γ_{stat}[d] /mN m^{-1}
F3H3-1	P($PFC_3GE^{0.20}$-*co*-$ME_3GE^{0.80}$)	02:08	20 [20]	28 [28]	2300 [2520]	1.11	21.67 ± 0.03
F3H3-2	P($PFC_3GE^{0.56}$-*co*-$ME_3GE^{0.44}$)	04:04	56 [50]	66 [61]	2700 [2320]	1.16	20.35 ± 0.03
F3H3-3	P($PFC_3GE^{0.27}$-*co*-$ME_3GE^{0.73}$)	04:08	27 [33]	36 [43]	2600 [3200]	1.07	21.94 ± 0.03
F3H3-4	P($PFC_3GE^{0.23}$-*co*-$ME_3GE^{0.77}$)	04:12	23 [25]	32 [34]	3900 [4080]	1.10	23.34 ± 0.03
F3H3-5	P($PFC_3GE^{0.12}$-*co*-$ME_3GE^{0.88}$)	04:24	12 [14]	17 [20]	4400 [6730]	1.09	25.02 ± 0.03
F3H3-6	P($PFC_3GE^{0.09}$-*co*-$ME_3GE^{0.91}$)	04:36	9 [10]	13 [15]	4500 [9370]	1.14	30.53 ± 0.03
F3B-1	$mPEG^{0.81}$-*b*-P(PFC_3GE)$^{0.19}$	13:04	19 [24]	64 [71]	1800 [1940]	1.10	21.51 ± 0.03
F3B-2	$mPEG^{0.76}$-*b*-P(PFC_3GE)$^{0.24}$	13:06	24 [32]	71 [78]	1900 [2620]	1.09	–[e]
F3B-3	$mPEG^{0.61}$-*b*-P(PFC_3GE)$^{0.39}$	13:13	39 [50]	83 [89]	2300 [5000]	1.12	–[e]
F3B-4	$mPEG^{0.94}$-*b*-P(PFC_3GE)$^{0.06}$[f]	50:04	6 [7]	33 [37]	2300[f] [3580]	1.41[f]	31.68 ± 0.03
F3B-5	$mPEG^{0.91}$-*b*-P(PFC_3GE)$^{0.09}$[f]	50:07	9 [12]	43 [51]	2500[f] [4600]	2.25[f]	28.53 ± 0.03
F3B-6	$mPEG^{0.97}$-*b*-P(PFC_3GE)$^{0.03}$[f]	123:04	3 [3]	19 [19]	4300[f] [6770]	1.10[f]	42.62 ± 0.03
F1H3-1	P($PFC_1GE^{0.29}$-*co*-$ME_3GE^{0.71}$)	02:04	29 [33]	31 [35]	1900 [1440]	1.09	25.61 ± 0.03
F1H3-2	P($PFC_1GE^{0.20}$-*co*-$ME_3GE^{0.80}$)	02:08	20 [20]	21 [21]	2200 [2320]	1.16	27.23 ± 0.03
F1H3-3	P($PFC_1GE^{0.16}$-*co*-$ME_3GE^{0.84}$)	02:12	16 [14]	17 [15]	3200 [3200]	1.11	29.22 ± 0.03
F1H3-4	P($PFC_1GE^{0.53}$-*co*-$ME_3GE^{0.47}$)	04:04	53 [50]	55 [52]	2000 [1920]	1.09	–[e]
F1H3-5	P($PFC_1GE^{0.33}$-*co*-$ME_3GE^{0.67}$)	04:08	33 [33]	35 [35]	2900 [2800]	1.09	25.23 ± 0.03
F1H3-6	P($PFC_1GE^{0.25}$-*co*-$ME_3GE^{0.75}$)	04:12	25 [25]	27 [27]	3300 [3680]	1.14	26.05 ± 0.03
F1H3-7	P($PFC_1GE^{0.14}$-*co*-$ME_3GE^{0.86}$)	04:24	14 [14]	15 [15]	5100 [6330]	1.13	31.79 ± 0.03
F1H3-8	P($PFC_1GE^{0.09}$-*co*-$ME_3GE^{0.91}$)	04:36	9 [10]	10 [11]	6100 [8970]	1.14	33.35 ± 0.03
F1H3-9	P($PFC_1GE^{0.48}$-*co*-$ME_3GE^{0.52}$)	06:06	48 [50]	50 [52]	2400 [2840]	1.10	–[e]
F1H3-10	P($PFC_1GE^{0.33}$-*co*-$ME_3GE^{0.67}$)	06:12	33 [33]	35 [35]	3600 [4160]	1.14	25.70 ± 0.03
F1H2-1	P($PFC_1GE^{0.22}$-*co*-$ME_2GE^{0.78}$)	02:08	22 [20]	35 [33]	2000 [1970]	1.08	26.92 ± 0.03
F1H2-2	P($PFC_1GE^{0.47}$-*co*-$ME_2GE^{0.53}$)	04:04	47 [50]	63 [66]	1600 [1750]	1.13	–[e]
F1H2-3	P($PFC_1GE^{0.35}$-*co*-$ME_2GE^{0.65}$)	04:08	35 [33]	51 [49]	2800 [2450]	1.08	26.54 ± 0.03
F1H2-4	P($PFC_1GE^{0.27}$-*co*-$ME_2GE^{0.73}$)	04:12	27 [25]	42 [39]	2600 [3160]	1.18	26.42 ± 0.03
F1H2-5	P($PFC_1GE^{0.15}$-*co*-$ME_2GE^{0.85}$)	04:24	15 [14]	25 [24]	3600 [5270]	1.15	28.41 ± 0.03
F1H2-6	P($PFC_1GE^{0.53}$-*co*-$ME_2GE^{0.47}$)	06:06	53 [50]	69 [66]	2400 [2580]	1.18	–[e]
F1H2-7	P($PFC_1GE^{0.33}$-*co*-$ME_2GE^{0.67}$)	06:12	33 [33]	49 [49]	3300 [3640]	1.09	26.36 ± 0.03

[a]Composition calculated from ^{1}H NMR spectroscopy (300 MHz, $CDCl_3$): x_F corresponds to mole fraction of fluorinated monomer in mol %, w_F corresponds to weight fraction of fluorinated monomer in wt %. [b]Theoretical DPs of fluorinated and hydrophilic monomers/components according to the feed ratio. A and B correspond to first and second components as listed in the systematic polymer description in column "Polymer". [c]Determined by SEC (RI detector, PEG standards). PFC_3GE-copolymers were measured in THF, PFC_1GE-copolymers in DMF as eluent. Values marked with "th" indicate theoretical values. [d]Surface tensions of 0.1 wt % aqueous solution measured with the Wilhelmy method. [e]Not analyzed for surface activity due to reduced solubility in aqueous media, indicated by turbidity of prepared solutions. [f]Incomplete initiation led to the formation of a blend composed of unmodified mPEG and the block copolymer.

and the lid was punctured to prevent bloating in case of gas formation. Thermal analysis was performed on second heating curve to remove adverse thermal history effects.

RESULTS AND DISCUSSION

Monomer Synthesis

To investigate polyethers as a potential scaffold for versatile fluorosurfactant design, a set of fluorine-containing monomers was devised. This was done conceptually by combining the polyfluorinated moieties featuring the −O−CHF−CF_2− motif, which was previously shown to facilitate degradation (*vide supra*), with an epoxide group required for polyether synthesis. Synthetically, such monomers are accessible by reacting perfluoroalkyl vinyl ethers with glycidol in a one-step base catalyzed addition reaction, giving rise to glycidyl ether monomers PFC_3GE and PFC_1GE (Figure 1) equipped with a terminal perfluorinated C3- or C1-unit, respectively.[29] Hydrophilic comonomers ME_2GE and ME_3GE were synthesized according to previously published methods.[39]

Surfactant Synthesis

Surfactants were synthesized via monomer-activated ring-opening polymerization (MAROP) of a mixture of amphiphobic and hydrophilic monomers, respectively. MAROP, first described by Deffieux and Carlotti,[40] serves as an alternative method to conventional anionic ring opening polymerization, allowing for a robust and straightforward synthesis under mild reaction conditions. It was therefore chosen as preferred synthetic strategy since the −O−CHF− moiety featured in PFC_1GE and PFC_3GE is susceptible to chemical breakdown under the strongly basic conditions typical for conventional AROP. All polymerizations were conducted in 2-methyltetrahydrofuran (2-MeTHF) as sustainable solvent.[41] 2-MeTHF is frequently used in MAROP since it does not induce catalyst deactivation typically observed for conventional THF.[42]

To investigate the effect of polymer composition and side chain architecture on the resulting surfactant performance, multiple series of copolymers were synthesized by varying the respective monomer combinations and feed ratios. Meanwhile, the targeted molar mass was kept below 10 000 g/mol throughout the entire study, since higher chain lengths were expected to negatively impact the dynamic surface activity of the surfactants.[43] An overview of all synthesized copolymers including ^{1}H NMR and SEC characterization data is given in Table 2.

As a starting point for our investigations, we first synthesized copolymers using PFC_3GE as the fluorinated monomer

https://doi.org/10.1021/acsapm.6c00173
ACS Appl. Polym. Mater. 2026, 8, 5101−5114

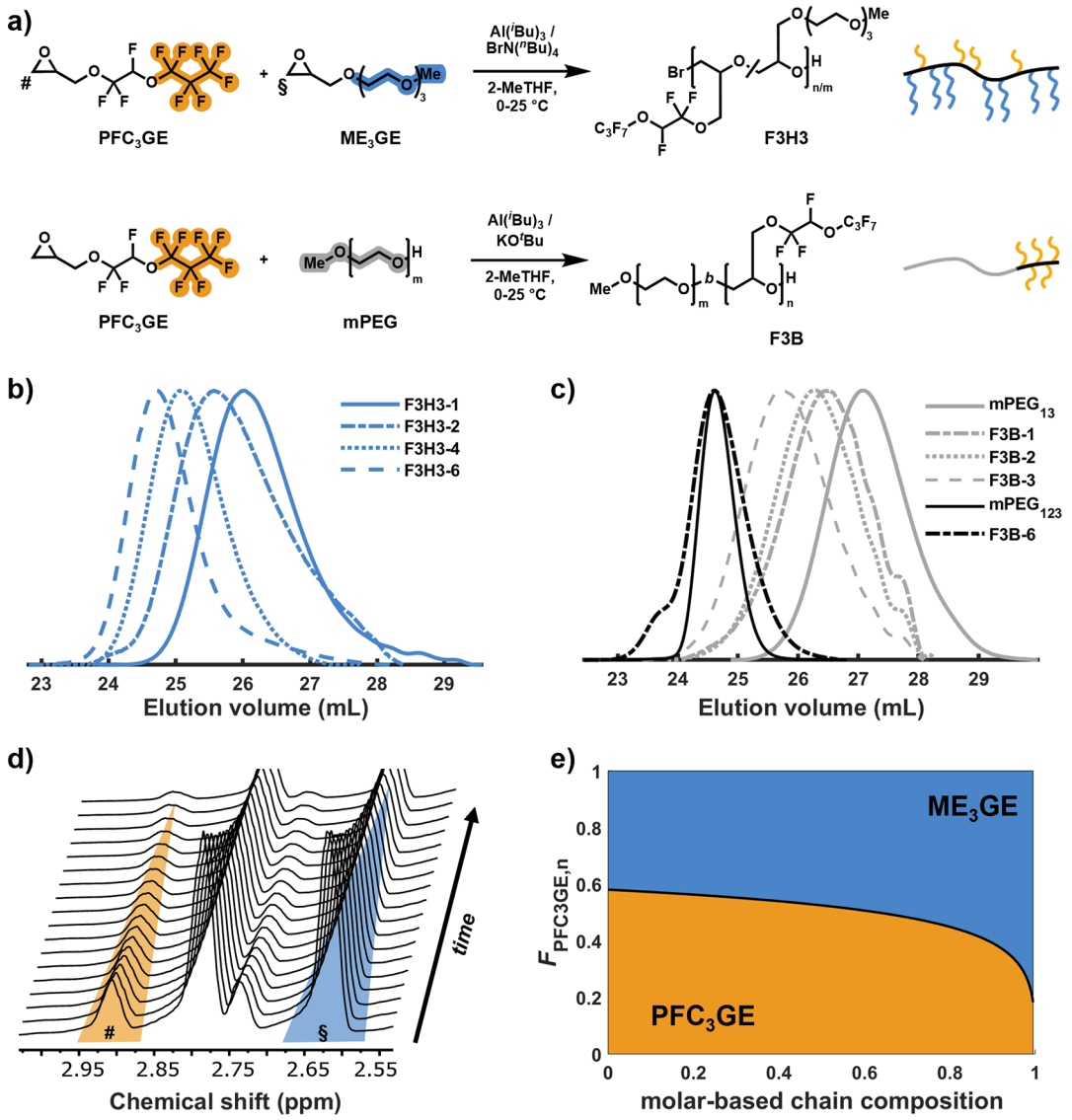

Figure 2. Synthesis and characterization of PFC_3GE-based fluorosurfactants: a) synthetic strategy toward P(PFC_3GE-*co*-ME_3GE) copolymers (top) as well as mPEG-*b*-P(PFC_3GE) block copolymers (bottom) via MAROP, b) selection of SEC traces (RI signals, eluent: THF) of P(PFC_3GE-*co*-ME_3GE) copolymers, c) selection of SEC traces (RI signals, eluent: THF) of mPEG-*b*-P(PFC_3GE) block copolymers, d) *in situ* ^1H NMR kinetic studies of the copolymerization toward P(PFC_3GE-*co*-ME_3GE) copolymers in 2-MeTHF. Zoomed-in region of monomer signals as a function of time. For both monomers, one of the methylene protons within the epoxide ring (indicated in a) with respective symbols) was used to derive the reactivity ratios, e) simulated chain composition profile for P(PFC_3GE-*co*-ME_3GE) copolymers based on the reactivity ratios of PFC_3GE and ME_3GE, exemplarily shown for 50 mol % PFC_3GE.

(Figure 2a, series F3H3 in Table 2). Through copolymerization with ME_3GE, copolymers featuring a statistical distribution of fluorinated and hydrophilic side chains were obtained. The targeted DPs were varied between 2−4 for PFC_3GE and 4−36 for ME_3GE, respectively. Meanwhile, targeted mole fractions of PFC_3GE were not raised above 50 mol % to reduce environmental impact and to warrant water solubility, which tends to decrease with increasing fluorine content. The experimental composition of the copolymers was verified via ^1H NMR spectroscopy and shows a high agreement with the targeted values. SEC characterization yielded low to moderate dispersities and monomodal molar mass distributions with a slight tailing to lower molar masses, which is typical for MAROP due to initiation side reactions (see Scheme S1, Supporting Information).[40,44] Generally, good agreement between theoretical and experimental number-average molar masses was observed. Discrepancies can be attributed to the PEG calibration, which shows different hydrodynamic radii than substituted polyethers. Sakakibara et al. reported an underestimation of the molar mass for polyethers with fluorinated side chains and attributed this to the high molar mass-volume ratio of fluorine atoms.[45] Here, discrepancies are observed mostly for higher targeted molar masses.

Besides statistical copolymers, the design of block copolymer structures based on PFC_3GE was also investigated (Figure 2a). Block copolymers represent attractive scaffolds for fluorosurfactant design, since a distinct spatial separation of hydrophilic and amphiphobic domains along the polymer backbone may enhance surface activity in solution. Polyether-based block copolymers are also well established in the design of conventional (nonfluorinated) surfactants.[46] In this study, block copolymers were synthesized through chain extension of

https://doi.org/10.1021/acsapm.6c00173
ACS Appl. Polym. Mater. 2026, 8, 5101−5114

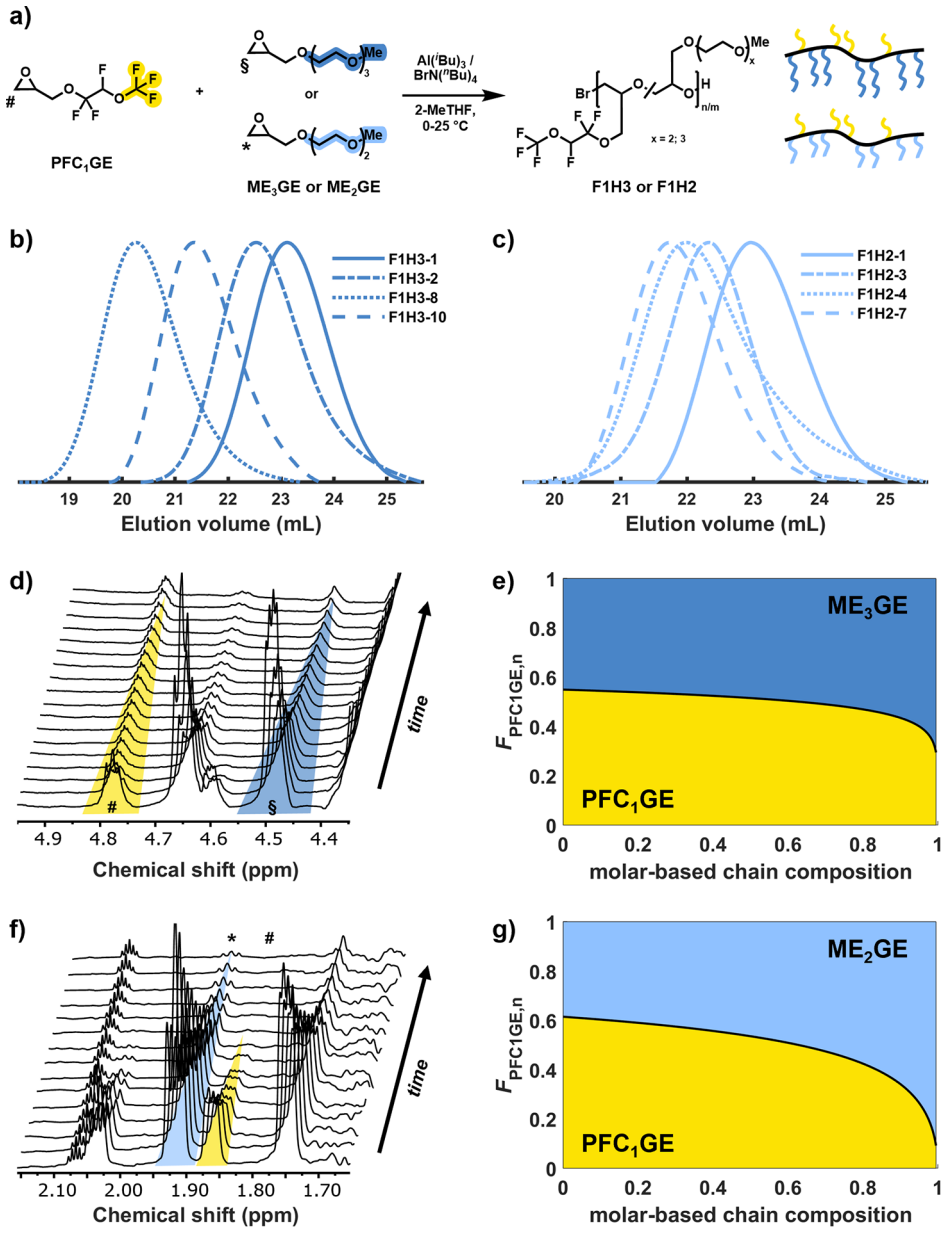

Figure 3. Synthesis and characterization of PFC_1GE-based fluorosurfactants: a) synthetic strategy toward P(PFC_1GE-*co*-ME_3GE) and P(PFC_1GE-*co*-ME_2GE) copolymers, respectively, b) selection of SEC traces (RI signals, eluent: DMF) of P(PFC_1GE-*co*-ME_3GE) copolymers, c) selection of SEC traces (RI signals, eluent: DMF) of Poly(PFC_1GE-*co*-ME_2GE) copolymers, d) and f) *in situ* ^1H NMR kinetic studies of the copolymerization toward P(PFC_1GE-*co*-ME_3GE) and P(PFC_1GE-*co*-ME_2GE), respectively, in 2-MeTHF. Zoomed-in region of monomer signals as a function of time. For both monomers, one of the methylene protons within the epoxide ring (indicated in a) with respective symbols) was used to derive the reactivity ratios, e) and g) simulated chain composition profiles for P(PFC_1GE-*co*-ME_3GE) and P(PFC_1GE-*co*-ME_2GE), respectively, based on the reactivity ratios of the corresponding monomers. Composition profiles are exemplarily shown for 50 mol % PFC_1GE.

mPEG macroinitiators (500, 2000, or 5000 g mol^{-1}, respectively) with PFC_3GE. For this, the macroinitiators were deprotonated with potassium *tert*-butoxide and polymerization was initiated after drying through the addition of fluorinated monomer. In contrast to the statistical copolymerizations shown previously, no TBAB initiator was added to avoid competing PFC_3GE homopolymerization. SEC analysis after workup revealed low dispersities for block copolymers based on $mPEG_{13}$ and $mPEG_{123}$ (Figure 2c). However, bimodal molar mass distributions were obtained in some cases, suggesting incomplete initiation by the mPEG alkoxide generated *in situ*. Proportions of unreacted mPEG in the product mixture tended to increase with the molar mass of macroinitiator used, so that in the case of $mPEG_{123}$, SEC analysis suggested that only a fraction of the macroinitiator underwent chain extension (also see Figure S2, Supporting Information). This might be due to several effects. First, the coil-like structure of the macroinitiator might impede further chain propagation through shielding of the active chain-end. Further, it was shown previously that MAROP polymerization kinetics scale inversely with the bulkiness of the cation, with alkali metal alkoxides such as potassium yielding much lower rate constants than the commonly used ammonium and phosphonium salts.[47] Indeed, synthesizing block copolymers via MAROP is known to be challenging, as incomplete crossover reactions can result in ill-defined product composi-

https://doi.org/10.1021/acsapm.6c00173
ACS Appl. Polym. Mater. 2026, 8, 5101−5114

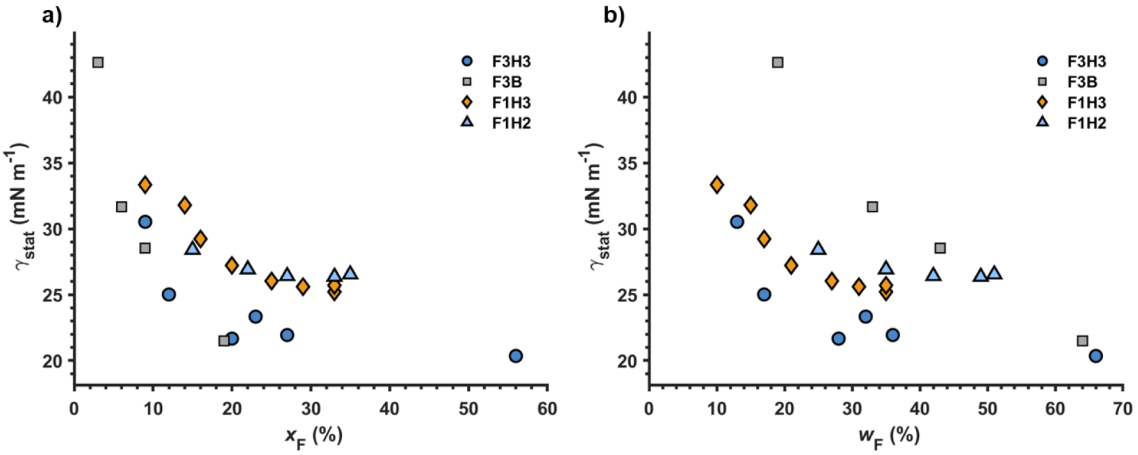

Figure 4. Static surface tension γ_{stat} of 0.1 wt % fluorosurfactant solutions as a function of copolymer composition: γ_{stat} plotted against a) number fraction x_F and b) mass fraction w_F of fluorinated monomer, respectively. Legend entries correspond to F3H3 – P(PFC_3GE-*co*-ME_3GE) (circles); F3B – mPEG-*b*-P(PFC_3GE) (blocks); F1H3 – P(PFC_1GE-*co*-ME_3GE) (diamonds); F1H2 – P(PFC_1GE-*co*-ME_2GE) (triangles).

tions. Consequently, only few reports exist on the successful preparation of such architectures by this method.[48−50] As for the block copolymers presented herein, successful chain extension (i.e., absence of PFC_3GE homopolymer formation) is verified via DOSY NMR spectroscopy (Figure S26) as well as a high agreement between targeted and experimental molar mass. For block copolymers based on $mPEG_{50}$, higher dispersities were obtained due to the more prominent second molar mass distribution in the SEC traces (Table 2, entries F3B-4 and F3B-5, Figure S2).

To investigate the effect of side-chain design on the resulting surfactant performance, studies were extended toward the synthesis of statistical copolymers based on PFC_1GE (Figure 3a). PFC_1GE is especially attractive from an ecological point of view, as the terminal perfluoromethyl group potentially allows for complete mineralization of the fluorine upon biodegradation, rather than producing ultra short-chain perfluorinated compounds as the terminal degradation product.[32] Taking into account the shorter fluorinated side chain of PFC_1GE, copolymerization was conducted with both ME_3GE and ME_2GE in two separate copolymer series (Table 2, series F1H3 and F1H2, respectively). To ensure comparability with previously synthesized P(PFC_3GE-*co*-ME_3GE) copolymers, the targeted degrees of polymerization (DP) were left unchanged. For both P(PFC_1GE-*co*-ME_3GE) copolymers as well as P(PFC_1GE-*co*-ME_2GE) copolymers, excellent agreement between theoretical and experimental comonomer composition and molar mass was observed. SEC analysis yielded monomodal and narrow molar mass distributions (Figure 3b and c, respectively).

Kinetic Investigation of the Polymerization

Generally, surface activity of statistical copolymers can be rationalized through intramolecular interactions between the different types of side chains involved, leading to mutual orientation of fluorinated and nonfluorinated segments in solution. We propose this to lead to an amphiphilic gradient perpendicular to the polymer backbone, enabling surface activity even for truly random copolymers ($r_1 = r_2 = 1$). Nevertheless, gradient and block-like architectures are expected to further support surface activity by creating predominantly hydrophilic and amphiphobic domains toward either end of the polymer chain, thus mimicking the structure commonly observed for small-molecule surfactants. To investigate the copolymer microstructure and its influence on surfactant performance, *in situ* ^{1}H NMR kinetic measurements of the polymerization processes toward P(PFC_3GE-*co*-ME_3GE), P(PFC_1GE-*co*-ME_3GE) and P(PFC_1GE-*co*-ME_2GE) were conducted. The polymerizations were performed in sealed Norell S5400 NMR tubes at 10 °C. For the reasons stated above, 2-MeTHF was used as the solvent for all copolymerizations, and an acetone-d_6 capillary was used for locking the spectrometer (for experimental details, see Supporting Information).

Figure 2d shows the decreasing monomer signals with time observed for the comonomer pair of PFC_3GE and ME_3GE. Kinetic evaluation of the respective integrals resulted in a slight incorporation preference of PFC_3GE, yielding reactivity ratios of $r_{PFC_3GE} = 1.38 \pm 0.05$ and $r_{ME_3GE} = 0.72 \pm 0.03$ using the nonterminal Jaacks model.[51] These results reflect an increased activation of the PFC_3GE toward nucleophilic attack, likely imparted by the electron-withdrawing nature of the fluorinated substituent. Thus, a soft gradient in the polymer microstructure is obtained, leading to a slight prevalence of fluorinated side chains toward one end of the polymer backbone. A simulated microstructure of P(PFC_3GE-*co*-ME_3GE) is displayed in Figure 2e. Reactivity values derived from the Jaacks model were in good agreement with the values calculated via BSL[52] and Meyer-Lowry ideal[53] (Table S3, see SI for kinetic models and plots). The product of the reactivity ratios equaling 1 further shows an ideal copolymerization behavior, meaning that the monomer addition is not influenced by the nature of the last added monomer unit.

Kinetic investigation of the copolymerization toward P(PFC_1GE-*co*-ME_3GE) yielded a similar microstructure, albeit with a slightly less pronounced gradient ($r_{PFC_1GE} = 1.22 \pm 0.04$ and $r_{ME_3GE} = 0.82 \pm 0.03$ via Jaacks). This can be ascribed to the slightly less electron withdrawing substituent of PFC_1GE, leading to a lower degree of activation than PFC_3GE. The progression of monomer signals with time as well as a simulated microstructure of P(PFC_1GE-*co*-ME_3GE) are shown in Figure 3d and e, respectively. In contrast, upon switching the hydrophilic comonomer to ME_2GE, a more pronounced gradient is observed, yielding $r_{PFC_1GE} = 1.60 \pm 0.02$ and $r_{ME_2GE} = 0.63 \pm 0.01$ (Figure 3e,f). This indicates that ME_3GE is more

https://doi.org/10.1021/acsapm.6c00173
ACS Appl. Polym. Mater. 2026, 8, 5101−5114

reactive than ME_2GE, presumably due to the higher number of oxygen atoms leading to a stronger complexation of the Lewis acid. Notably, Herzberger et al. found an opposing trend for the comonomer pair of ethylene oxide and ethoxy ethyl glycidyl ether, albeit under slightly different reaction conditions.[44]

In a further study, the copolymerization of ME_3GE and PFC_3GE was examined in THF as a cheaper and more industrially relevant solvent. In this case, an excess of TIBAL was required to achieve sufficient conversion (19 equiv. with respect to TBAB). Kinetic evaluation revealed a slightly more pronounced gradient compared to 2-MeTHF with reactivity ratios of $r_{PFC_3GE} = 1.54 \pm 0.01$ and $r_{ME_3GE} = 0.65 \pm 0.01$, suggesting that ME_3GE reactivity is further reduced through competitive catalyst complexation by THF. These results demonstrate that copolymerization in THF is generally feasible, though significantly higher amounts of activator are required compared to weaker-coordinating solvents.

Surface Tension

Static and dynamic surface tension measurements were conducted to assess both the equilibrium and time-dependent interfacial behavior of the synthesized polymeric surfactants.

Static Surface Tension

The static surface tension was measured using the Wilhelmy method on 0.1 wt % aqueous polymer solutions in equilibrium.[54] The results are listed in Table 2. As discussed above, the relative amount of fluorinated monomer (PFC_1GE or PFC_3GE, respectively) with respect to the total number of repeat units per polymer was calculated from ^1H NMR analysis of the obtained polymer sample. Here, this number fraction x_F serves as a measure to assess (i) the environmental burden of a given surfactant imparted by the amount of fluorine it contains, and (ii) the predominant surfactant properties through its ratio of amphiphobic and hydrophilic segments (analogously to the HLB value introduced for nonfluorinated polymer-based surfactants).[55] A graphical representation of the static surface tension γ_{stat} of the synthesized copolymer surfactants against x_F is given in Figure 4.

As a general trend throughout all copolymer series, it is evident that the static surface tension decreases with increasing fluorine content of the polymer. This is a commonly observed phenomenon since larger hydrophobic segments within the surfactant tend to promote its assembly at the air−water interface through repulsive interactions with the aqueous medium.[56−58] Interestingly, Sharma et al. observed an opposing trend on statistical copolymers featuring fluorotelomer and oligo(ethylene glycol) side chains and attributed this to steric hindrance at the phase boundary.[59] Meanwhile, when comparing copolymers F1H3-1, F1H3-5 and F1H3-10 as well as F1H2-3 and F1H2-7, each featuring a similar fluorine content but varying molar masses, strikingly similar γ_{stat} values were obtained. Therefore, we propose that within the low molar mass regime targeted in this study, surfactant performance in equilibrium is predominantly dictated by molar composition rather than average molar mass of the polymer.

When comparing the different copolymer series, it can be observed that all statistical copolymers display a continuous γ_{stat} decrease with increasing x_F, eventually reaching a plateau value. Of these, P(PFC_3GE-*co*-ME_3GE) copolymers displayed the lowest surface tension of 20.35 mN/m (x_F = 56%). In contrast, P(PFC_1GE-*co*-ME_3GE) copolymers reached a plateau at roughly 25 mN/m, indicating the shorter fluorinated side chain of PFC_1GE to be slightly less surface active than its longer pendant. Note that no PFC_1GE-based copolymers with $x_F > 35\%$ could be analyzed for their surface activity due to reduced solubility in water, most likely caused by predominantly hydrophobic character of the overall structure. To account for the shorter polyfluorinated side chain of PFC_1GE compared to PFC_3GE (featuring 6 vs 10 fluorine atoms, respectively), γ_{stat} was also plotted against the weight fraction of fluorinated monomer w_F (Figure 4b). When comparing P(PFC_3GE-*co*-ME_3GE) and P(PFC_1GE-*co*-ME_3GE) copolymers in Figure 4b, it is evident that the former still display superior surface activity, though differences are less pronounced. For low weight fractions of $w_F \leq 20\%$, γ_{stat} progressions for copolymers based on PFC_3GE and PFC_1GE initially follow a similar trajectory. Importantly, this suggests that a loss in surface activity caused by shorter (i.e., more environmentally benign) perfluorinated segments may, to a certain degree, be compensated for by the addition of more such segments to the polymer backbone.

In copolymers based on PFC_1GE, hydrophilic comonomers ME_3GE as well as ME_2GE were investigated to account for the shorter terminal fluoroalkyl group of PFC_1GE. However, substituting ME_3GE with ME_2GE did not result in a significant change in equilibrium surface activity.

Block copolymers mPEG-*b*-P(PFC_3GE) display a sharp decrease of surface tension with increasing PFC_3GE content (gray rectangles in Figure 4), reaching 21.51 mN m^1 at x_F = 19% (F3B-1). These results are competitive toward surface tensions of P(PFC_3GE-*co*-ME_3GE) copolymers obtained at significantly higher molar PFC_3GE contents (x_F = 56%, F3H3-2) which might indicate a positive influence of the polymer architecture on surface activity.[43] Another possible explanation stems from the fact that in the case of mPEG-*b*-P(PFC_3GE), relatively low DP of PFC_3GE correspond to high w_F due to the low molar mass of EO repeat units (Figure 4b). For block copolymers synthesized from $mPEG_{13}$ with $x_F \geq 24\%$, decreased aqueous solubility was observed due to predominantly hydrophobic character of the polymers.

In a broader perspective, the copolymers presented herein show comparable surface activity to previously published polymer-based fluorosurfactants.[43,59,60] The copolymers with highest surface activity further proved competitive toward the legacy compounds perfluorooctanesulfonic acid ($\gamma_{stat} \geq 21.9$ mN m^{-1})[5] and sodium perfluorooctanoate ($\gamma_{stat} \geq 24.7$ mN m^{-1})[5] as well as modern commercial fluorosurfactants such as TIVIDA FL 2300 (Merck KGaA, $\gamma_{stat} \geq 21.1$ mN m^{-1})[61] and 3M FC-4430 (3M, $\gamma_{stat} \geq 23$ mN m^{-1}).[62] On the other hand, the copolymers did not achieve the surface activity of TIVIDA FL 2500 ($\gamma_{stat} \geq 18.0$ mN m^{-1})[61] or FL 2700 ($\gamma_{stat} \geq 16.8$ mN m^{-1}).[63]

Dynamic Surface Tension

The dynamic surface tension of a nonequilibrium system was measured using the maximum bubble pressure method on 0.1 wt % aqueous solutions.[64] When a new interface is formed, surfactant molecules gradually migrate and adsorb at the interface, resulting in a decrease in interfacial tension. This relaxation process involves several mechanistic steps, including diffusion, reorientation, and adsorption of surfactant molecules, leading to a time-dependent approach toward equilibrium.[59,65] Unlike the static surface tension, which reflects the overall efficacy of a given surfactant, dynamic measurements provide insight into its ability to achieve rapid surface

https://doi.org/10.1021/acsapm.6c00173
ACS Appl. Polym. Mater. 2026, 8, 5101−5114

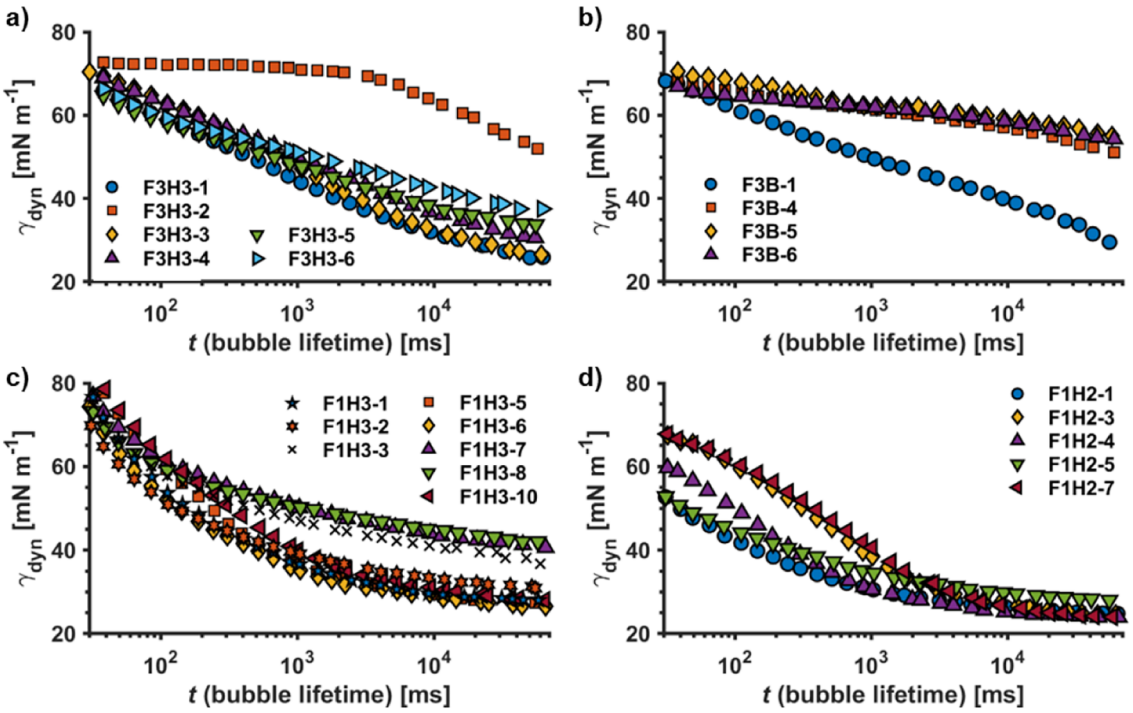

Figure 5. Dynamic surface tension of a) P(PFC_3GE-*co*-ME_3GE), b) mPEG-*b*-P(PFC_3GE), c) P(PFC_1GE-*co*-ME_3GE) and d) P(PFC_1GE-*co*-ME_2GE) copolymers from 0.1 wt % aqueous solutions.

relaxation through fast equilibration kinetics.[66] This is especially important for applications featuring time-dependent processes such as spray painting, high-speed coating and printing, and inkjet applications.,[38,67,68] Polymer-based fluorosurfactants generally show slower equilibration than their small-molecule counterparts due to more complex rearrangement processes required at the phase boundary.[38,59]

Figure 5 shows the dynamic surface tension γ_{dyn} plotted against the bubble lifetime for all copolymers where sufficient solubility was observed (Table 2). When comparing the γ_{dyn} profiles of the statistical copolymers (Figure 5a,c and d), it is evident that PFC_3GE-based copolymers generally exhibit slower equilibration kinetics than copolymers synthesized from PFC_1GE. Hence, for all P(PFC_3GE-*co*-ME_3GE) copolymers (Figure 5a), dynamic surface tensions measured after 60 s are higher than their corresponding γ_{stat} values obtained from the Wilhelmy method (see Table S1, Supporting Information). This indicates incomplete equilibration within the investigated time frame, which can be attributed to slower rearrangement processes of the long PFC_3GE side chains at the interface.[59] This is especially evident in the case of F3H3-2, where an initial induction period of ∼3 s is observed until the surface tension starts to decline. We hypothesize this to be caused by competing micellization processes in solution, promoted by the exceptionally high fluorine content and resulting hydrophobicity of the copolymer (x_F = 56%).

For mPEG-*b*-P(PFC_3GE) copolymers, an almost linear decrease of surface tension is observed (Figure 5b). Except for F3B-1, which was synthesized from a low molar mass precursor ($mPEG_{13}$), all block copolymers possess markedly slow equilibration kinetics. None of the samples reached their corresponding equilibrium surface tensions within the investigated time frame. We initially expected the block polymer architecture to support dynamic surface activity by enabling a faster reorientation process at the interface.[43] However, these results suggest that a distinct spatial separation of hydrophilic and amphiphobic segments within the polymer architecture does not necessarily induce fast equilibration kinetics. In the case of block copolymers F3B-4 to F3B-6, slow equilibration might be caused by the long, coil-like hydrophilic tails ($mPEG_{50}$ and $mPEG_{123}$, respectively), hindering fast diffusion and conformational arrangement in solution.

For P(PFC_1GE-*co*-ME_3GE) copolymers, a markedly faster reduction in surface tension was observed as compared to P(PFC_3GE-*co*-ME_3GE) copolymers (Figure 5c). Dynamic surface tensions measured after 60 s are in good agreement with γ_{stat} results obtained previously. However, copolymers F1H3-3, F1H3-7 and F1H3-8 did not reach full equilibration within the investigated time frame, likely due to their lower fluorine content ($x_F \leq 16\%$) and consequently reduced hydrophobicity. Replacing the hydrophilic comonomer ME_3GE by the shorter ME_2GE (Figure 5d) led to lower γ_{dyn} on short time scales, which can be attributed to faster conformational rearrangements at the interface enabled by short amphiphobic and hydrophilic side chains.

DEGRADATION STUDIES

For established fluorosurfactants based on perfluorinated structural motifs, biodegradation is typically limited to the nonfluorinated part of the molecule, leaving the fluorocarbon chain essentially unaltered.[69,70] This degradation pathway significantly contributes to the ecological burden imparted by all PFAS through the gradual buildup of perfluorinated residues in the environment.[10] Industrial PFAS disposal is challenging and requires highly cost-intensive processes such as incineration at >1000 °C or electrochemical oxidation due to the exceptional stability of the C−F bond (*vide supra*).[19,20]

To verify the general degradability of the fluorinated moieties presented herein, a simple experimental setup was devised. In this, PFC_1GE homopolymer was subjected to basic

https://doi.org/10.1021/acsapm.6c00173
ACS Appl. Polym. Mater. 2026, 8, 5101−5114

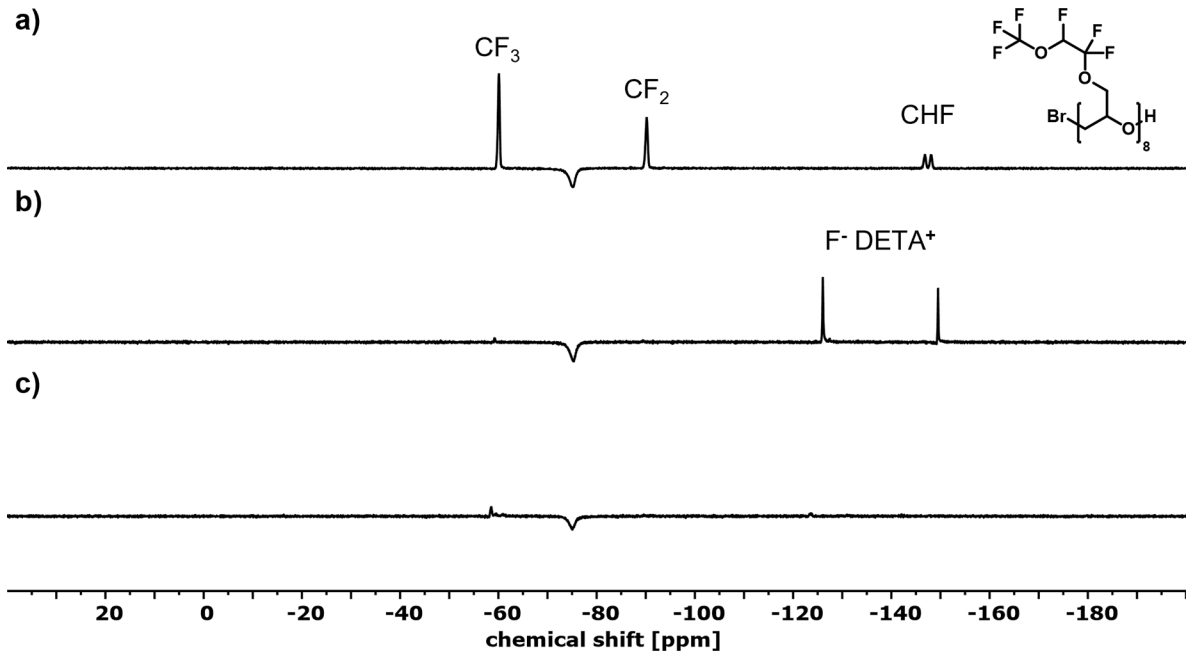

Figure 6. Degradation studies on P(PFC_1GE) conducted under basic conditions in DMSO-d_6 at 120 °C: a) ^{19}F NMR spectrum of P(PFC_1GE) before degradation, b) ^{19}F-NMR spectrum after degradation using diethylenetriamine (DETA) as base taken after 6 days, and c) ^{19}F NMR spectrum after degradation using potassium hydroxide as base taken after 5 days. Here, no signals corresponding to decomposition products are observable due to precipitation of fluoride salt from the reaction medium. Negative signals at −75 ppm correspond to transmitter breakthrough artifacts.

conditions by adding diethylenetriamine or KOH at 120 °C and conversion was monitored via ^{19}F NMR spectroscopy (Figure 6 as well as Figures S29 and S30, Supporting Information). Depending on experimental conditions, degradation to terminal CF_3O^- species or complete mineralization was observed within few days. This proof-of-concept exemplifies that PFC_1GE- and PFC_3GE-based copolymers require significantly less energy-intensive decomposition processes compared to legacy PFAS. In light of extensive degradation studies previously conducted on structurally similar compounds, the copolymers presented herein are promising candidates for advanced degradation experiments under environmentally relevant conditions. These will be the focus of future studies.

CONCLUSION

A set of fluorinated epoxide monomers, PFC_3GE and PFC_1GE, was developed by combining degradable polyfluorinated moieties featuring the −O−CHF−CF_2− motif with glycidyl functionality for polyether synthesis. Using monomer-activated anionic ring-opening polymerization (MAROP), surfactants were prepared either through statistical copolymerization with hydrophilic comonomers ME_3GE or ME_2GE, or by synthesizing block copolymers through chain extension of mPEG macroinitiators. Both the overall fluorine content as well as the polymer molar mass could be systematically varied simply by adjusting the monomer feed. Kinetic investigations revealed soft gradient polymer architectures for all statistical copolymers.

Upon tensiometric analysis, surface activity was found to be influenced significantly by polymer architecture and overall fluorine content of the copolymers. Statistical copolymers based on PFC_3GE and PFC_1GE reached equilibrium surface tensions of 20 mN m^{-1} (x_F = 56%) and 25 mN m^{-1} (x_F = 33%), respectively. This renders the polymer-based fluorosurfactants competitive toward the legacy compound perfluorooctanesulfonic acid (21.9 mN m^{-1}) and sodium perfluorooctanoate (24.7 mN m^{-1}) as well as some modern commercial fluorosurfactants. No significant influence of polymer molar mass on the surface activity was observed. Notably, it was found that a loss in surface activity imparted by shorter (i.e., more environmentally benign) fluorinated side chains may partially be offset by increasing the feed ratio of fluorinated monomer. Dynamic surface tension measurements revealed relatively slow equilibration kinetics, particularly for PFC_3GE-based copolymers, as is typically observed for polymer-based surfactants due to more complex rearrangement processes required at the phase boundary.

Degradability of the polyfluorinated side chains was examined in a simple experimental setup under basic conditions on PFC_1GE homopolymer, and degradation to terminal perfluorinated moiety or complete mineralization was observed after few days. Previous studies on similar compounds suggest that the surfactants presented herein are also susceptible to breakdown under biologically relevant conditions, reducing the environmental burden imparted by these fluorosurfactants.

In a broader perspective, the results presented herein highlight the potential of innovative strategies for the development of more sustainable fluorosurfactants. Considering increasingly restrictive PFAS regulations, fluorosurfactants with an improved degradation profile and comparable performance might represent a valuable addition to the product landscape. This is especially true for those applications, where nonfluorinated alternatives do not yet qualify as a suitable replacement for PFAS products, or where there is an increased risk of leaching into the environment.

https://doi.org/10.1021/acsapm.6c00173
ACS Appl. Polym. Mater. 2026, 8, 5101−5114

These include aqueous fire-fighting foams (AFFF), (architectural) paints and coatings and electronics.

■ ASSOCIATED CONTENT

Supporting Information

The Supporting Information is available free of charge at https://pubs.acs.org/doi/10.1021/acsapm.6c00173.

Experimental details, MAROP polymerization mechanism, NMR analytical data of monomers and polymer-based surfactants, SEC curves of copolymers, MALDI-ToF spectra of PFC_1GE homopolymer and copolymer, DSC analysis of PFC_1GE and PFC_3GE homopolymers, SST and DST results of all surfactants in tabular format, chemical degradation studies, supplementary *in situ* ^1H NMR kinetic data of all statistical copolymerizations (PDF)

■ AUTHOR INFORMATION

Corresponding Author

Holger Frey − *Johannes Gutenberg-Universität Mainz, Department of Chemistry, 55128 Mainz, Germany;* orcid.org/0000-0002-9916-3103; Email: hfrey@uni-mainz.de

Authors

Tom Reimers − *Johannes Gutenberg-Universität Mainz, Department of Chemistry, 55128 Mainz, Germany*

Larissa Limmer − *Johannes Gutenberg-Universität Mainz, Department of Chemistry, 55128 Mainz, Germany*

Gregor M. Linden − *Johannes Gutenberg-Universität Mainz, Department of Chemistry, 55128 Mainz, Germany*

Johannes Liermann − *Johannes Gutenberg-Universität Mainz, Department of Chemistry, 55128 Mainz, Germany*

Reiner Friedrich − *Merck KGaA, 64293 Darmstadt, Germany*

Complete contact information is available at: https://pubs.acs.org/10.1021/acsapm.6c00173

Author Contributions

T.R. and L.L. contributed equally to this work. All authors have given approval to the published version of the manuscript. T.R.: Investigation, Data Curation, Interpretation, Visualization, Writing (Original Draft, Review and Editing). L.L.: Conceptualization, Investigation, Data Curation, Interpretation, Writing (Original Draft). G.M.L.: Investigation (Support in Acquisition and Evaluation of NMR Kinetic Data), Writing (Review and Editing). J.L.: Investigation (Technical Support in Acquisition of NMR Kinetic Data). R.F.: Conceptualization, Interpretation and Discussion of Experimental Data, Investigation (Acquisition of Static and Dynamic Surface Tension Data, Degradation Analysis), Writing (Review). Holger Frey: Conceptualization, Funding Acquisition, Supervision, Writing (Review).

Notes

The authors declare no competing financial interest.

■ ACKNOWLEDGMENTS

The authors thank Merck KGaA for scientific collaboration and for providing the fluorine-containing compounds PFC_3GE and PMVE. The authors thank Sabine Hennig for practical support, Elena Berger-Nicoletti for MALDI-ToF measurements, and Tobias Gäb for assistance in graphical design.

■ REFERENCES

(1) Quéré, D. Non-sticking drops. *Rep. Prog. Phys.* **2005**, *68* (11), 2495−2532.

(2) Kim, H.-A. Water Repellency/Proof/Vapor Permeability Characteristics of Coated and Laminated Breathable Fabrics for Outdoor Clothing. *Coatings* **2022**, *12* (1), 12.

(3) *Fluorinated surfactants and repellents*, Surfactant science series, 2rd ed.; Marcel Dekker, Vol. *97*, 2001.

(4) Capstone *C Online Brochure: Capstone Fluorosurfactants:For high value-in-use applications that require maximum performance.* https://www.chemours.com/en/-/media/files/capstone/capstone-surfactants-brochure.pdf.

(5) Peshoria, S.; Nandini, D.; Tanwar, R. K.; Narang, R. Short-chain and long-chain fluorosurfactants in firefighting foam: a review. *Environ. Chem. Lett.* **2020**, *18* (4), 1277−1300.

(6) Jochyms, Q.; Mignard, E.; Vincent, J.-M. Fluorosurfactants for applications in catalysis. *J. Fluorine Chem.* **2015**, *177*, 11−18.

(7) Banerjee, S.; Tawade, B. V.; Ladmiral, V.; Dupuy, L. X.; MacDonald, M. P.; Améduri, B. Poly(fluoroacrylate)s with tunable surface hydrophobicity via radical copolymerization of 2,2,2-trifluoroethyl α-fluoroacrylate and 2-(trifluoromethyl)acrylic acid. *Polym. Chem.* **2017**, *8* (12), 1978−1988.

(8) O'Hagan, D. Understanding organofluorine chemistry. An introduction to the C-F bond. *Chem. Soc. Rev.* **2008**, *37* (2), 308−319.

(9) Cousins, I. T.; Johansson, J. H.; Salter, M. E.; Sha, B.; Scheringer, M. Outside the Safe Operating Space of a New Planetary Boundary for Per- and Polyfluoroalkyl Substances (PFAS). *Environ. Sci. Technol.* **2022**, *56* (16), 11172−11179.

(10) Evich, M. G.; Davis, M. J. B.; McCord, J. P.; Acrey, B.; Awkerman, J. A.; Knappe, D. R. U.; Lindstrom, A. B.; Speth, T. F.; Tebes-Stevens, C.; Strynar, M. J.; Wang, Z.; Weber, E. J.; Henderson, W. M.; Washington, J. W. Per- and polyfluoroalkyl substances in the environment. *Science* **2022**, *375* (6580), No. eabg9065.

(11) Bartell, S. M.; Vieira, V. M. Critical review on PFOA, kidney cancer, and testicular cancer. *J. Air Waste Manage Assoc.* **2021**, *71* (6), 663−679.

(12) Fenton, S. E.; Ducatman, A.; Boobis, A.; DeWitt, J. C.; Lau, C.; Ng, C.; Smith, J. S.; Roberts, S. M. Per- and Polyfluoroalkyl Substance Toxicity and Human Health Review: Current State of Knowledge and Strategies for Informing Future Research. *Environ. Toxicol. Chem.* **2020**, *40* (3), 606−630.

(13) Wang, Z.; Cousins, I. T.; Scheringer, M.; Hungerbuehler, K. Hazard assessment of fluorinated alternatives to long-chain perfluoroalkyl acids (PFAAs) and their precursors: status quo, ongoing challenges and possible solutions. *Environ. Int.* **2015**, *75*, 172−179.

(14) U.S. Environmental Protection Agency. *Fact Sheet: 2010/2015 PFOA Stewardship Program.* https://www.regulations.gov/docket/EPA-HQ-OPPT-2006-0621.

(15) European Union *Regulation (EU) 2019/1021 of the European Parliament and of the Council of 20 June 2019 on persistent organic pollutants (POPs Regulation)*; European Union, 2019.

(16) Ameduri, B. What Do We Know About Per- or Polyfluoroalkyl Substances (PFASs)? Issues, Challenges, Regulations, and Possible Alternatives. *Macromolecules* **2025**, *58* (6), 2781−2791.

(17) Pérez, F.; Nadal, M.; Navarro-Ortega, A.; Fàbrega, F.; Domingo, J. L.; Barceló, D.; Farré, M. Accumulation of perfluoroalkyl substances in human tissues. *Environ. Int.* **2013**, *59*, 354−362.

(18) Pickard, H. M.; Criscitiello, A. S.; Persaud, D.; Spencer, C.; Muir, D. C. G.; Lehnherr, I.; Sharp, M. J.; Silva, A. O. D.; Young, C. J. Ice Core Record of Persistent Short-Chain Fluorinated Alkyl Acids: Evidence of the Impact From Global Environmental Regulations. *Geophys. Res. Lett.* **2020**, *47* (10), No. e2020GL087535.

(19) Winchell, L. J.; Ross, J. J.; Wells, M. J. M.; Fonoll, X.; Norton, J. W.; Bell, K. Y. Per- and polyfluoroalkyl substances thermal destruction at water resource recovery facilities: A state of the science review. *Water Environ. Res.* **2021**, *93* (6), 826−843.

(20) Smith, S. J.; Lauria, M.; Ahrens, L.; McCleaf, P.; Hollman, P.; Bjälkefur Seroka, S.; Hamers, T.; Arp, H. P. H.; Wiberg, K. Electrochemical Oxidation for Treatment of PFAS in Contaminated Water and Fractionated Foam-A Pilot-Scale Study. *ACS EST Water* **2023**, *3* (4), 1201−1211.
(21) Hori, H.; Nagano, Y.; Murayama, M.; Koike, K.; Kutsuna, S. Efficient decomposition of perfluoroether carboxylic acids in water with a combination of persulfate oxidant and ultrasonic irradiation. *J. Fluorine Chem.* **2012**, *141*, 5−10.
(22) Hori, H.; Murayama, M.; Kutsuna, S. Oxygen-induced efficient mineralization of perfluoroalkylether sulfonates in subcritical water. *Chemosphere* **2009**, *77* (10), 1400−1405.
(23) OECDPer- and Polyfluoroalkyl Substances and Alternatives in Coatings, Paints and Varnishes (CPVs): Report on the Commercial Availability and Current Uses
(24) Joudan, S.; Mabury, S. A. Aerobic biotransformation of a novel highly functionalized polyfluoroether-based surfactant using activated sludge from a wastewater treatment plant. *Environ. Sci. Process Impacts* **2022**, *24* (1), 62−71.
(25) Joudan, S.; Orlando, J. J.; Tyndall, G. S.; Furlani, T. C.; Young, C. J.; Mabury, S. A. Atmospheric Fate of a New Polyfluoroalkyl Building Block, C3F7OCHFCF2SCH2CH2OH. *Environ. Sci. Technol.* **2022**, *56* (10), 6027−6035.
(26) Folkerson, A. P.; Joudan, S.; Mabury, S. A.; D'eon, J. C. In Vivo Transformation of a Novel Polyfluoroether Surfactant. *Environ. Toxicol. Chem.* **2021**, *40* (12), 3328−3336.
(27) Houde, M.; Martin, J. W.; Letcher, R. J.; Solomon, K. R.; Muir, D. C. G. Biological monitoring of polyfluoroalkyl substances: A review. *Environ. Sci. Technol.* **2006**, *40* (11), 3463−3473.
(28) Sadrabadi, F.; Alker, W.; Sprenger, H.; Braeuning, A.; Buhrke, T. A group of novel polyfluoroether substances affects lipid metabolism in human hepatocyte HepaRG cells less than classic perfluoroalkyl compounds. *Toxicol. In Vitro* **2025**, *105*, 106024.
(29) Changoer, L.; Anastassov, G. Suppositories comprising cannabinoids; WO 2,018,075,730 A1, 2017.
(30) Herzberger, J.; Niederer, K.; Pohlit, H.; Seiwert, J.; Worm, M.; Wurm, F. R.; Frey, H. Polymerization of Ethylene Oxide, Propylene Oxide, and Other Alkylene Oxides: Synthesis, Novel Polymer Architectures, and Bioconjugation. *Chem. Rev.* **2016**, *116* (4), 2170−2243.
(31) Folkerson, A. P.; Mabury, S. A. A Comparative Biodegradation Study to Assess the Ultimate Fate of Novel Highly Functionalized Hydrofluoroether Alcohols in Wastewater Treatment Plant Microcosms and Surface Waters. *Environ. Toxicol. Chem.* **2024**, *43*, 2297.
(32) Folkerson, A. P.; Schneider, S. R.; Abbatt, J. P. D.; Mabury, S. A. Avoiding Regrettable Replacements: Can the Introduction of Novel Functional Groups Move PFAS from Recalcitrant to Reactive? *Environ. Sci. Technol.* **2023**, *57* (44), 17032−17041.
(33) Liu, X.-H.; Meng, T.-T.; Ni, S.; Zhao, Z.; Bai, F.-Y. Kinetic and mechanistic study of the atmospheric degradation of C3F7OCHFCF2SCH2CH2OH with OH radical. *Chem. Phys. Lett.* **2023**, *823*, 140516.
(34) Lv, G.; Yang, J.; Sun, X.; Wang, G.; Cheng, Z.; Yang, Z.; Xu, C.; Cai, J.; Xu, X. Understanding the atmospheric transformation mechanism of an emerging fluorinated alcohol (FESOH). *Atmos. Environ.* **2023**, *309*, 119903.
(35) Kredel, J.; Gallei, M. Ozone-Degradable Fluoropolymers on Textile Surfaces for Water and Oil Repellency. *ACS Appl. Polym. Mater.* **2020**, *2* (7), 2867−2879.
(36) Hintzer, K.; Kaspar, H.; Schwertfeger, W.; Heinfeldner, R. Process for producing fluoropolymers; US 20,100,227,992 A1, 2010.
(37) Lindstrom, A. B.; Strynar, M. J.; Libelo, E. L. Polyfluorinated compounds: past, present, and future. *Environ. Sci. Technol.* **2011**, *45* (19), 7954−7961.
(38) Schuster, T.; Krumpfer, J. W.; Schellenberger, S.; Friedrich, R.; Klapper, M.; Müllen, K. Effects of chemical structure on the dynamic and static surface tensions of short-chain, multi-arm nonionic fluorosurfactants. *J. Colloid Interface Sci.* **2014**, *428*, 276−285.
(39) Wang, M.; Wang, E.; Cao, H.; Liu, S.; Wang, X.; Wang, F. Construction of Self-Reporting Biodegradable CO2-Based Polycarbonates for the Visualization of Thermoresponsive Behavior with Aggregation-Induced Emission Technology. *Chin. J. Chem.* **2021**, *39* (11), 3037−3043.
(40) Billouard, C.; Carlotti, S.; Desbois, P.; Deffieux, A. "Controlled" High-Speed Anionic Polymerization of Propylene Oxide Initiated by Alkali Metal Alkoxide/Trialkylaluminum Systems. *Macromolecules* **2004**, *37* (11), 4038−4043.
(41) Jordan, A.; Hall, C. G. J.; Thorp, L. R.; Sneddon, H. F. Replacement of Less-Preferred Dipolar Aprotic and Ethereal Solvents in Synthetic Organic Chemistry with More Sustainable Alternatives. *Chem. Rev.* **2022**, *122* (6), 6749−6794.
(42) Roos, K.; Carlotti, S. Grignard-based anionic ring-opening polymerization of propylene oxide activated by triisobutylaluminum. *Eur. Polym. J.* **2015**, *70*, 240−246.
(43) Alaimo, D.; Beigbeder, A.; Dubois, P.; Broze, G.; Jérôme, C.; Grignard, B. Block, random and palm-tree amphiphilic fluorinated copolymers: controlled synthesis, surface activity and use as dispersion polymerization stabilizers. *Polym. Chem.* **2014**, *5* (18), 5273−5282.
(44) Herzberger, J.; Leibig, D.; Liermann, J. C.; Frey, H. Conventional Oxyanionic versus Monomer-Activated Anionic Copolymerization of Ethylene Oxide with Glycidyl Ethers: Striking Differences in Reactivity Ratios. *ACS Macro Lett.* **2016**, *5* (11), 1206−1211.
(45) Sakakibara, K.; Nakano, K.; Nozaki, K. Regioregular Polymerization of Fluorine-Containing Epoxides. *Macromolecules* **2007**, *40* (17), 6136−6142.
(46) Pitto-Barry, A.; Barry, N. P. E. Pluronic® block-copolymers in medicine: from chemical and biological versatility to rationalisation and clinical advances. *Polym. Chem.* **2014**, *5* (10), 3291−3297.
(47) Labbé, A.; Carlotti, S.; Billouard, C.; Desbois, P.; Deffieux, A. Controlled High-Speed Anionic Polymerization of Propylene Oxide Initiated by Onium Salts in the Presence of Triisobutylaluminum. *Macromolecules* **2007**, *40* (22), 7842−7847.
(48) Brocas, A.-L.; Gervais, M.; Carlotti, S.; Pispas, S. Amphiphilic diblock copolymers based on ethylene oxide and epoxides bearing aliphatic side chains. *Polym. Chem.* **2012**, *3* (8), 2148.
(49) Carlotti, S.; Labbé, A.; Rejsek, V.; Doutaz, S.; Gervais, M.; Deffieux, A. Living/Controlled Anionic Polymerization and Copolymerization of Epichlorohydrin with Tetraoctylammonium Bromide−Triisobutylaluminum Initiating Systems. *Macromolecules* **2008**, *41* (19), 7058−7062.
(50) Rejsek, V.; Sauvanier, D.; Billouard, C.; Desbois, P.; Deffieux, A.; Carlotti, S. Controlled Anionic Homo- and Copolymerization of Ethylene Oxide and Propylene Oxide by Monomer Activation. *Macromolecules* **2007**, *40* (18), 6510−6514.
(51) Jaacks, V. A Novel Method of Determination of Reactivity Ratios in Binary and Ternary Copolymerizations. *Makromol. Chem.* **1972**, *161* (1), 161−172.
(52) Beckingham, B. S.; Sanoja, G. E.; Lynd, N. A. Simple and Accurate Determination of Reactivity Ratios Using a Nonterminal Model of Chain Copolymerization. *Macromolecules* **2015**, *48* (19), 6922−6930.
(53) Meyer, V. E.; Lowry, G. G. Integral and differential binary copolymerization equations. *J. Polym. Sci.* **1965**, *3* (8), 2843−2851.
(54) Volpe, C. D.; Siboni, S. The Wilhelmy method: a critical and practical review. *Surf. Innovat.* **2018**, *6* (3), 120−132.
(55) Griffin, W. C. Classification of Surface-Active Agents by "HLB". *J. Soc. Cosmet. Chem.* **1949**, *1* (5), 311−326.
(56) Yoshimura, T.; Ohno, A.; Esumi, K. Equilibrium and dynamic surface tension properties of partially fluorinated quaternary ammonium salt gemini surfactants. *Langmuir* **2006**, *22* (10), 4643−4648.
(57) Patel, R.; Saab, L. E.; Brahana, P. J.; Valsaraj, K. T.; Bharti, B. Interfacial Activity and Surface pKa of Perfluoroalkyl Carboxylic Acids (PFCAs). *Langmuir* **2024**, *40* (7), 3651−3658.

(58) Wei, B.; Guo, X.; Cui, Y.; Ma, S.; Li, W.; Bai, Y. Polyether fluorinated amphiphilic diblock polymer: Preparation, characterization and application as drug delivery agent. *Eur. Polym. J.* **2022**, *162*, 110872.
(59) Sharma, S. C.; Acharya, D. P.; García-Roman, M.; Itami, Y.; Kunieda, H. Phase behavior and surface tensions of amphiphilic fluorinated random copolymer aqueous solutions. *Colloids Surf., A* **2006**, *280* (1−3), 140−145.
(60) Song, L.; Wang, R.; Niu, K.; Liu, Y.; Kou, J.; Song, H.; Zhang, J.; Wang, Q. Design, synthesis, characterization, and surface activities of comb-like polymeric fluorinated surfactants with short fluoroalkyl chains. *Colloids Surf., A* **2021**, *609*, 125666.
(61) Merck KGa, A. *Tivida® FL: Highly effective fluorosurfactants for better spreading and leveling on surfaces*. https://www.emdgroup.com/Products/PM/us/Tivida-FL-effective-fluorosurfactants-US.pdf (accessed 10 October 2025).
(62) *Technical Datasheet 3M Fluorosurfactant FC-4430*. https://geoconproducts.com/pdf_download/TDS/FC_4430.pdf (accessed 20 October 2025).
(63) Merck *technical datasheet 1.40013 Tivida® FL 2700*; Merck, 2018.
(64) Fainerman, V. B.; Miller, R. Maximum bubble pressure tensiometry—an analysis of experimental constraints. *Adv. Colloid Interface Sci.* **2004**, *108−109*, 287−301.
(65) Zhmud, B. V.; Tiberg, F.; Kizling, J. Dynamic Surface Tension in Concentrated Solutions of C n E m Surfactants: A Comparison between the Theory and Experiment. *Langmuir* **2000**, *16* (6), 2557−2565.
(66) Guo, Y.; Yao, C. Polyether- and Tertiary Amine-Modified Silicone Surfactants: Synthesis and Surface Performance Across pH Ranges. *Polymers* **2025**, *17* (9), 1204.
(67) Rump, M.; Diddens, C.; Sen, U.; Versluis, M.; Lohse, D.; Segers, T. Role of surfactants in droplet formation in piezoacoustic inkjet printing across microsecond-to-second timescales. *Phys. Rev. Appl.* **2025**, *23* (2), 024076.
(68) Rogren, P. E. Three-dimensional, additive manufacturing system, and a method of manufacturing a three-dimensional object; US 20,200,108,553 A1, 2021.
(69) Moody, C. A.; Field, J. A. Perfluorinated Surfactants and the Environmental Implications of Their Use in Fire-Fighting Foams. *Environ. Sci. Technol.* **2000**, *34* (18), 3864−3870.
(70) Key, B. D.; Howell, R. D.; Criddle, C. S. Fluorinated Organics in the Biosphere. *Environ. Sci. Technol.* **1997**, *31* (9), 2445−2454.

https://doi.org/10.1021/acsapm.6c00173
ACS Appl. Polym. Mater. 2026, 8, 5101−5114